Trapping and sorting of active matter in a periodic background potential

H. E. Ribeiro,[1,*] W. P. Ferreira,[2,†] and Fabrício Q. Potiguar[1,‡]

[1]*Universidade Federal do Pará, Faculdade de Física, ICEN, Avenida Augusto Correa 1, Guamá, 66075-110 Belém, Pará, Brazil*

[2]*Departamento de Física, Universidade Federal do Ceará, Campus do Pici, 60455-760 Fortaleza, Ceará, Brazil*

(Received 22 November 2019; accepted 21 February 2020; published 19 March 2020)

We study, numerically, a system of active particles with either a single noise value or a mixture of equal proportions of particles with two noise values under the influence of an attractive periodic background potential, and we observe their diffusion regimes and trapping states. For the single noise system, we show that the slow diffusion is correlated to a significant particle trapping, while normal diffusion is seen for partial or no trapping. Our results indicate that low noise particles are less susceptible to the background, i.e., they have a smaller chance to be trapped as compared to higher noise particles for the same background, and that denser systems achieve a no-trapping state, unless for the largest noise value we studied. For the mixtures, we study the sorting of particles based on their noise value differences and observe that particles with distinct noises are trapped at distinct radii compared to a trap minimum, and, since these radii depend on the density, the latter should be well tuned in order to have an efficient sorting.

DOI: 10.1103/PhysRevE.101.032126

I. INTRODUCTION

Active (or self-propelled) particles, man-made or biological, are entities which produce (or absorb) energy for their motion, usually in a random direction [1]. Numerical models are largely employed aiming to understand the effect of collective motion [2], clustering [3], phase separation [4], and, recently, manipulation [5]. Several reported results in the literature show how to capture active particles [6] and rectify their motion [7,8] in a lattice of traps, mimicking the dynamics on a crystalline surface [9]. Further, promising studies related to the control of such particles by imposing obstacles [10], external fields [11], and boundaries [12] are expanding the branches of research in self-motile dynamics.

Recently, it was shown numerically [13] that active rods can be trapped inside a V-shaped rigid boundary, a structure much used in probing net transport [7]. Such trapping depends on the particle density, φ, and the angle of the V, α, and occurs in three regimes: no trapping, in which $\alpha \geqslant 120^{\circ}$ and it is virtually independent of φ; complete trapping, for $\alpha_L \leqslant \alpha \leqslant 120^{\circ}$, with α_L dependent on φ; and partial trapping, which occurs for $\alpha \leqslant \alpha_L$. All three phases meet at a triple point such that, for higher φ, the complete trapping phase is suppressed, implying that the V barrier has a saturation limit. Also, Kumar *et al.* [14] showed through experiments and simulations for the same type of barrier that one can sort mixtures of active rods based on the rotational noise difference between the species, respecting, obviously, the limits imposed by the barrier; they showed that lower noise particles tend to get trapped while those of larger noise fly about. In these investigations, the confinement is purely a geometrical effect [6]; the particles cannot cross the arms of the V since the potential is infinite. We proposed to investigate the same phenomenon but for a soft boundary and see what changes occur to such trapping patterns. Our soft boundary will be provided by an external potential that mimics an optical tweezer. We call it a soft trap or well.

The technique of optical tweezers is a powerful tool to manipulate [15–20] matter in a noninvasive way, as part of the main scenario of manipulation techniques at the microscale and nanoscale. The attractive background generated by the set of focused laser beams forms one of the various examples of patterned substrates explored in theoretical and experimental realizations. Therefore, we investigate the dynamics of an active system in the presence of a periodic potential background, made of a square lattice of attractive wells, mimicking a similar lattice of optical tweezers. We will refer to the potential minima (and the regions around them) simply as wells. Previous works showed that passive particles under such background potential can be seen to realize the lattice gas model [16], have focused on sorting [17] either induced by size [18] or index of refraction [19], and showed that, when driven by a constant external flow, particles tend to follow specific directions of motion when passing through such background [20]. In the present paper, we do not take into account variations in particle shape. Instead, we examine the interplay of the effective density of the system to active fluctuations on the particle dynamics, insofar as the attractive regions select a kind of particle whereas the other one may pass, by adjusting the strength of the wells. We measured two quantities through which we characterize our findings: the mean square displacement (MSD), averaged over all particles and realizations, and the fraction of trapped particles (FTP) in a well. The second was already used as a measure for the classification of the trapping transition [13,14].

*he.ribeiro@bol.com.br

†wandemberg@fisica.ufc.br

‡fqpotiguar@ufpa.br

Our paper has a close correspondence to Refs. [21,22] in the use of soft traps. However, we have three major differences of implementation.

(1) We studied a lattice of soft traps, as opposed to a single trap.

(2) As a consequence of this first choice, motivated by various studies with passive particles in such backgrounds [16–20], we considered smaller trap radii, not larger than three particle diameters, than those of Refs. [21,22], around 30 particle diameters.

(3) Our traps, in general, do not have circular boundaries of constant force, as for a parabolic trap.

Finally, we investigated sorting mixtures of active particles with distinct noise values, as in Ref. [14], using such a setup, where Ref. [22] investigated the same phenomenon but for a passive-active particle mixture. Given these differences, our paper follows a line of investigation closer to that of Refs. [13,14], namely, classification of trapping transition, but bearing a link, its relation to diffusion, to the works of Refs. [21,22].

The paper is organized as follows. In Sec. II, we present the numerical model. In Sec. III, we present the results for trapping and sorting. Lastly, in Sec. IV, we present our conclusions.

II. MODEL

Our setup follows the approach of Ref. [3] and consists of soft, interacting self-propelled disks, which are free to move on a two-dimensional (2D) periodic array of attractive wells. The dynamics of the ith disk is governed by the coupled overdamped Langevin equations, i.e.,

$$\begin{aligned}\frac{\partial \mathbf{r}_i}{\partial t} &= v_i + \mu[\mathbf{F}_i - \nabla_i U(\mathbf{r})] + \boldsymbol{\xi}_i(t),\\ \frac{\partial \theta_i(t)}{\partial t} &= \eta_i(t),\end{aligned} \tag{1}$$

where $\mathbf{r}_i$ is the position of the ith particle and $\theta_i(t)$ is the direction of the intrinsic velocity vector $v_i = v_0[\cos\theta_i(t)\hat{i} + \sin\theta_i(t)\hat{j}]$, v_0 being its magnitude. The Gaussian white noises $\boldsymbol{\xi}_i(t)$ and $\eta_i(t)$ represent the thermal fluctuations, from ordinary Brownian motion, and active fluctuations (due to some inner mechanism of the particles) responsible for changing the internal motion direction, respectively. Both have zero mean and their correlations are given by $\langle \xi_{ia}(t)\xi_{jb}(t')\rangle = 2D_t\delta_{ij}\delta_{ab}\delta(t-t')$ and $\langle \eta_i(t)\eta_j(t')\rangle = 2D_r\delta_{ij}\delta(t-t')$, with intensities D_t (translational diffusion coefficient) and D_r (rotational diffusion coefficient), $i, j = 1, \ldots, N$, and $a, b = x, y$. The term $F_i = \sum_{j\neq i} F_{ij}$, where $F_{ij} = \kappa a_{ij}\hat{r}_{ij}$ for $a_{ij} > 0$ ($F_{ij} = 0$ otherwise), accounts for the soft interaction among particles, with $a_{ij} = (\frac{d}{2} - r_{ij})$ and d their diameters. The parameter $\mu = 1$ is the mobility. The initial values for positions and velocities directions are random, both updated at time increments $\Delta T = 0.001$. The system is allowed to evolve for $t/\Delta T = 3\times 10^6$ cycles, in which 10^6 of those cycles are considered as thermalization cycles where no measurements are performed. We neglected hydrodynamic interactions and thermal fluctuations [3], i.e., our model is entirely non-Brownian (we do this by setting $D_t = 0$). In single noise systems, we used $D_r = 10^{-5}, 10^{-2}, 1.0$, and 10. For the binary system we considered two mixtures: $D_r = 10^{-5}$ and 10, and $D_r = 10^{-2}$ and 1.0, both with equal proportions. Other fixed parameters are interparticle interaction stiffness $\kappa = 10$ and self-propulsion velocity magnitude $v_0 = 1$. Lengths are given in units of d, while the time unit is set by $t = d/v_0$, with $v_0 = 1$. We considered three distinct densities $\varphi = 0.1, 0.2$, and 0.3 in order to check for their influence on the change of the trapping of particles.

The periodic background is modeled by the 2D potential

$$U(x,y) = \frac{-V_0}{1 + \exp\left[-A\left(\cos\left(\frac{2\pi x}{\lambda}\right) + \cos\left(\frac{2\pi y}{\lambda}\right) - 2B\right)\right]}, \tag{2}$$

which generates a force field very similar to that of a lattice of optical tweezers [17]. The parameter B stands for the relative size of the wells. The larger the values of B the narrower the wells. In our setup, $B = [0.1\text{–}1]$. The parameter $A = 5$. The space available for the particles is chosen according to the lattice spacing λ. We define a square box with $L_x = L_y = 96$, so that we have 13×13 periodic wells spaced by $\lambda = 8$ such that periodic boundary conditions are correctly implemented. The potential strength V_0 sets the residence time (t_{trap}), i.e., the average time a particle spends within a single well. Once inside a well, a particle has a larger chance to escape for lower values of V_0 for a fixed λ. Simulations are carried out for $V_0 = 2.0$.

Finally, we discuss briefly the role of the distinct time scales of our setup. One of them is the usual active motion time scale $t_r = 1/D_r$, which defines the diffusion regime; given our background potential, we define an escape time scale as $t_e = R/v_0$, in which R stands for the distance between the well center and the boundary around it in which the maximum restoring force is below v_0/μ (see below for a more detailed discussion). This expression may be seen as the amount of time a noiseless particle starting from a well center covers a distance of R. The value of R is closely related to the parameter B of the potential (as implied above); the largest R value we considered was about $R \approx 3$; given the value of the self-propulsion speed, we have that the escape time scale is of the order of $t_e = 1$ time unit. We ran our simulations for times of the order of 10^3 time units, which far surpasses t_e. Therefore, we believe to have passed any transient effects related to escaping the wells. We discuss the role of t_r below.

III. RESULTS AND DISCUSSIONS

A. Trapping in single noise systems

We begin by showing our MSD results. Given that we have an attractive background potential, we would expect the influence of such potential to show up in the long time limit of these curves. For instance, if we have a state in which this influence is minimal, we would expect to see normal, or even faster, diffusion. On the other hand, given that this influence is considerable, we would probably have subdiffusion; clearly, for the complete trapping state, we would have no diffusion, or maybe strong subdiffusion as seen in Refs. [21,22]. In Fig. 1, we show the MSD for all φ, D_r, and B values we studied. Clearly, we have several distinct diffusion regimes ranging from ballistic to normal to no diffusion (plateaus) with no

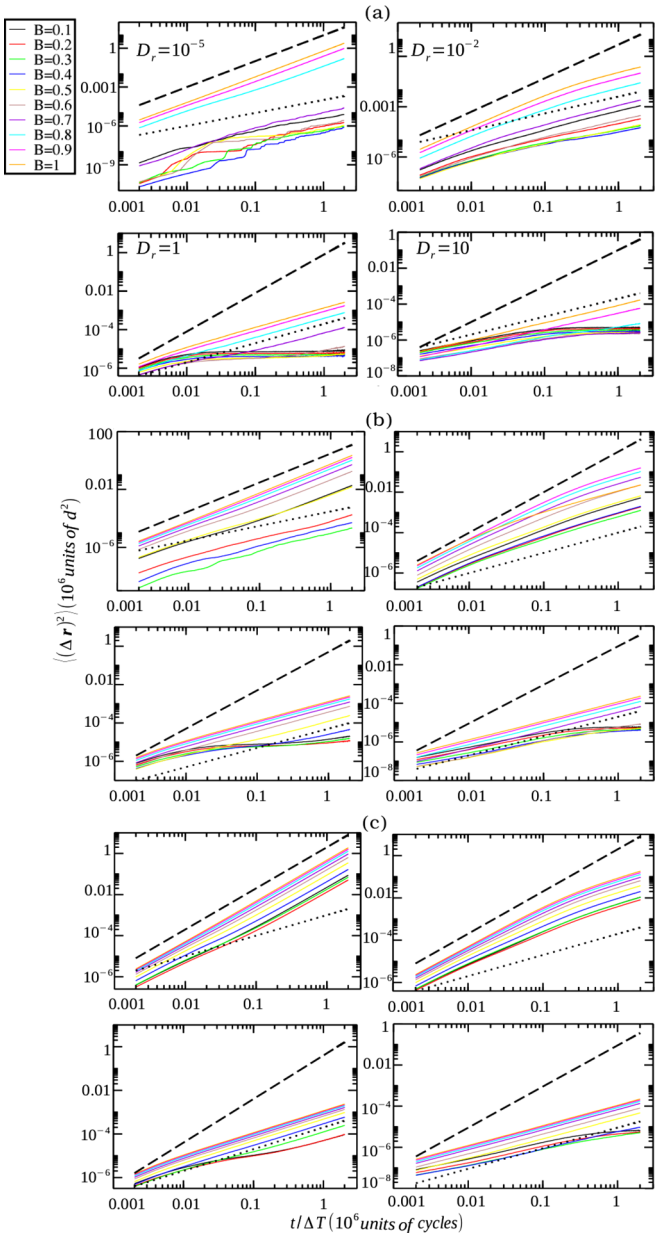

FIG. 1. The MSD for (a) $\varphi = 0.1$, (b) $\varphi = 0.2$, and (c) $\varphi = 0.3$ as a function of time, given in cycles, for different values of parameter B. The background strength and length are $V_0 = 2$ and $\lambda = 8$. The dotted and dashed lines scale as t and t^2, respectively.

apparent discontinuous changes among them. There is even evidence of cage effects, in which we see an intermediate no-diffusion state between the limit behaviors of the MSD.

We see that for fixed φ and D_r, for $B \geqslant 0.8$, the diffusion regime is either ballistic for low noise or normal. For now, let us concentrate on the curves for $D_r \geqslant 10^{-2}$; we will return to the results for $D_r = 10^{-5}$ after commenting on the results for the FTP. As we decrease B, the long time MSD curves progressively change from normal to plateaus for $D_r \geqslant 1.0$; for $D_r = 10^{-2}$ there is no appreciable change in the regime. If we fix φ and B, the change in the diffusion regime with D_r is more pronounced, always from faster to slower diffusion, with increasing D_r, for lower B. This indicates that there is a trend for particle trapping to occur at high noise, and larger wells (lower B), as seen by the plateaus at $D_r = 1.0$ and 10.

For fixed D_r and B, increasing the particle density makes the system less susceptible to the external potential, i.e., the diffusion become faster for larger densities. For instance, for $B = 0.6$ and $D_r = 10$, we have at $\varphi = 0.1$ a trapped state, while at $\varphi = 0.2$ this plateau is barely visible, and we have a regime close to normal diffusion; finally, at $\varphi = 0.3$, normal diffusion is evident. As a distinct example, take the $B = 0.4$ curve at $D_r = 1.0$. We see that it shows nearly a trapped state at $\varphi = 0.1$; for the next density, the MSD clearly shows a cage effect, but reaching normal diffusion; finally, at $\varphi = 0.3$, we only have normal diffusion. It is customary to show single particle trajectories to characterize the system state, but in this case such correlation does not occur because, since we consider a particle to be trapped if it stays in a well for a definite amount of time, in a system partially trapped, for instance, there will be both types of trajectories, those that remain a long time in a well and those that do not. Hence, single particle trajectories are a not a good indicator of the trapping state.

Our findings, hence, indicate that high noise particles are more easily trapped compared to the low noise ones; also, larger wells trap particles more easily; finally, adding more particles to the system makes it less affected by the external potential. The first feature is different from what was reported in Refs. [13,14] for hard traps; in their investigations, the opposite occurred: high noise particles are less probable to get trapped. This is the effect of their rigid boundary, in what we called earlier a geometrical effect. Since low noise particles have a longer persistent motion, i.e., they travel a longer distance before changing drastically their direction of motion as compared to the high noise ones, when inside a rigid V barrier, this longer path will eventually reach the apex of the V, since active particles slide along solid surfaces; given many such particles entering the inner part of the V, it will be nearly impossible for the particles to turn their motion around and escape a trap for a proper apex angle. Also, as a contingent feature of their investigations, the shapes of the particles (rods) are very suited to be trapped in their V boundaries; there is even the appearance of orientational order in the trapped state [13]. In our case, given that we have a soft boundary, such features should not play a very important role in the results.

The long persistent motion is precisely what makes the active disks less susceptible to the external potential given the soft boundary [21–24]. To see this consider that an isolated active particle with no thermal motion will always cross a barrier if its maximum restoring force is less than v_0/μ. Hence, we have simply a force balance condition to determine whether escaping an attractive well will occur. This is in contrast to recent studies of the generalized Kramers problem [25–27], where the escape rate is calculated for active particles with thermal fluctuations. This force condition alone is not enough, though, for the crossing to occur because the particle, starting from a well center, must climb the potential barrier up to the point of maximum restoring force and keep its motion beyond it in order to escape the well. For a given well radius, i.e., a B value, particles with a higher D_r will have lower probabilities of reaching such a point and will be

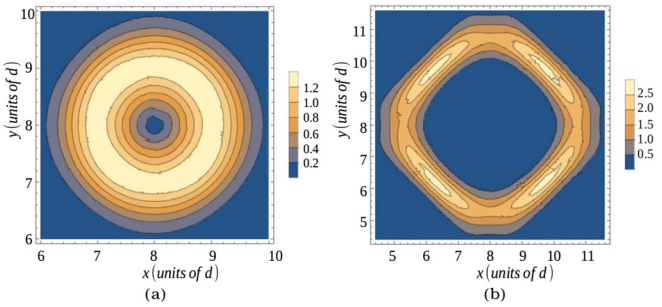

FIG. 2. Contour plot of the gradient force $\vec{F} = -\nabla U(x, y)$ for $V_0 = 2$ and (a) $B = 0.9$ and (b) $B = 0.2$.

trapped in this well. Therefore, the rotational noise should be low, given that the force balance condition is satisfied, so that a particle may escape a well. Our investigation was carried out for a system of interacting particles, therefore this isolated particle picture is changed in a way that particles with high noise reach the points of maximum restoring force by being pushed inside a well by others. This scenario helps to understand the dependence of the diffusion regime as we increase particle density: by adding more particles, more of them will be captured by the wells, but more of them will interact; hence, given an appropriating density, high noise particles may reach the maximum restoring force boundary more easily, increasing their chance for escaping. Also, the escaping could occur even if the maximum restoring force condition is not met for an individual particle, regardless of its noise value: if it is pushed more strongly by the others against the maximum restoring force, it will escape. As a comparison, in a recent study of a collection of passive particles under such periodic potentials [28,29], the main effect of increasing density, at particle number commensurate to the number of potential minima, at fixed temperature is to produce several distinctly ordered configurations of particles within each minima, but no escape is induced unless the temperature is large enough.

This whole scenario does not hold for our largest well radii $B \leqslant 0.3$. Our results for these values deviate from the general behavior described here; these MSD curves show a stronger diffusion than for smaller wells. Specifically, when we have $D_r = 10^{-2}$ and $\varphi \leqslant 0.2$, we see that the MSD curves decrease their absolute values for decreasing B, but the curves below $B = 0.3$ increase with decreasing B (which can also be seen for $D_r = 1.0$ and and 10 at these densities). This occurs because, in general, the well has a circular shape for large B [see Fig. 2(a)]; as B decreases, these circles disappear, and the maximum restoring force occurs only in particular directions [see Fig. 2(b) for an example in which this maximum force is along the $\pm\pi/4$ related to the horizontal]. Hence, particles can escape these wells more easily through the paths along the main directions, where the force is lower, leading to such strange behaviors. The average density field for $\varphi = 0.1$, $D_r = 10^{-2}$, and $B = 0.1$ seen in Fig. 3(a) clearly shows such "escape routes" for these strongest wells. Perhaps, these features could be avoided by using simpler background potentials, such as the harmonic traps of Refs. [21–23], but we do feel that our general conclusions regarding the trapping

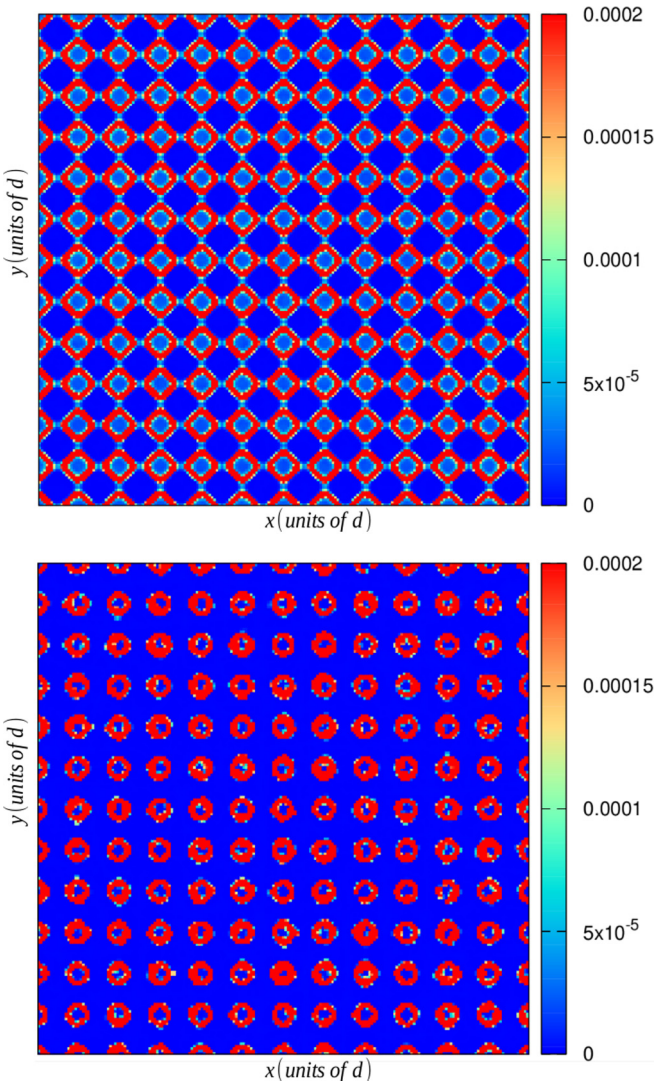

FIG. 3. Time-averaged density map measured for $\varphi = 0.1$. The parameters are (a) $B = 0.1$ and $D_r = 10^{-2}$ and (b) $B = 0.4$ and $D_r = 10^{-5}$.

phenomenon and the diffusion regimes are independent of such potentials.

All of these conclusions were made based solely on the MSD results. Still, we cannot, except in some very evident cases, say whether we have no, partial, or complete trapping, according to the classification of Ref. [13]. We already have a few hints on such states: the normal ones are probably those of no or partial trapping, while the plateaus correspond to complete trapping states; all the other regimes, including the caged states, may be an instance of the partial trapping state. In the end, a precise classification can only be made with the values for the FTP. We show in Fig. 4 this quantity, as an average over all particles, for all the parameters used. To measure such fraction, we follow the particles, after the thermalization time, and measure the time they spend in a well. The well boundary is the circle around a well minimum that passes over the farthest point in which the restoring force is $\leqslant v_0/\mu$. If this time is equal to the simulation time, then it is trapped. Note that this is a strong requirement to make;

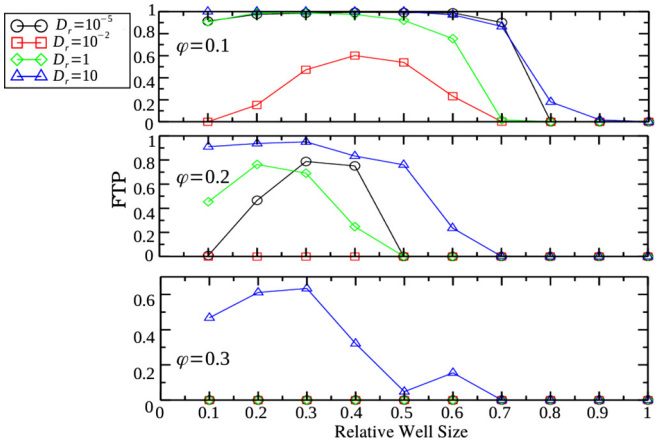

FIG. 4. The fraction of trapped particles as a function of the relative well size B for all D_r and φ.

particles should enter a well and not leave it for the whole simulation (in Ref. [13], the trapping time for a particle was taken at a much lower value). We show, in Fig. 5, the mean distribution of the maximum residence time, $P(t_m)$, of a single particle within a well for $D_r = 10^{-2}$ and 1.0, $B = 0.4$, and all φ; other cases have similar results for this quantity. The $P(t_m)$ is computed by, at the end of each realization, measuring for each particle the longest time it remained in a single well and constructing $P(t_m)$ from these data as an average over all particles and realizations.

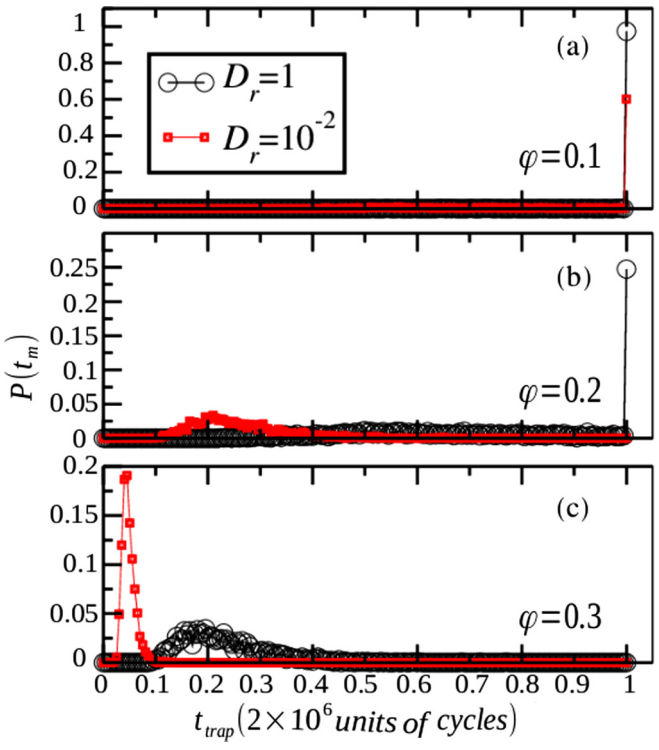

FIG. 5. Maximum residence time distribution $P(t_m)$ for $D_r = 10^{-2}$ and 1.0; $B = 0.4$; (a) $\varphi = 0.1$; (b) $\varphi = 0.2$; and (c) $\varphi = 0.3$ (these are representative of the whole phenomenon). The horizontal axis is normalized by the simulation time in each case.

Let us begin with the results for $\varphi = 0.1$. We see that, for $D_r = 10^{-2}$ and 1.0, there is a progressive increase of the FTP for $B \leqslant 0.7$ until $B = 0.4$. For lower B, the FTP decreases (which is an effect of the distorted well boundary, as remarked earlier). For $D_r = 10$, there is a similar trend, but the FTP begins to increase for $B \leqslant 0.8$. We see that the cases in which there are no trapped particles, i.e., in which the FTP is zero, are correlated with normal or superdiffusion curves of Fig. 1(a); in the cases in which the FTP is near 1, there is no diffusion. Note that for $\varphi = 0.1$, Fig. 5(a), we have partial trapping for $D_r = 10^{-2}$ (given the peak at $t_m = 1$) and total trapping for $D_r = 1.0$ (seen as the sharp peak at $t_m = 1$).

When we consider the results for the other two density values, $\varphi = 0.2$ and 0.3, we see that there is a similar trend of the FTP with B: it is zero for large B, and increases at some definite B, until decreasing again. The main effect, though, of increasing the particle density is that the FTP magnitude decreases. It is an effect similar to what was reported in Refs. [13,14], where the authors go from a total trapping to a partial trapping state by increasing φ. At $\varphi = 0.2$, Fig. 5(b), we see that the $P(t_m)$ for $D_r = 10^{-2}$ has broadened around $t_m = 0.20$, and no particle is trapped according to our condition, hence the vanishing of the FTP for this case. For $D_r = 1.0$, the sharp peak at $t_m = 1$ is much lower and there is a broad peak around $t_m = 0.50$, characterizing partial trapping. Finally, at $\varphi = 0.3$, Fig. 5(c), at $D_r = 10^{-2}$, there is only one narrow peak around $t_m = 0.30$, i.e., there is no trapping; for $D_r = 1.0$ the data have broadened between $t_m = 0.10$ and 0.40. This is another evidence that an active particle trap, either hard or soft, has a saturation point where total trapping will cease to occur. In our case, this saturation point is a function of the background intensity V_0 and angular noise. We passed through all three trapping regimes by only increasing the density. This is rather surprising, since at $\varphi = 0.1$, as reported in Refs. [21,22], there are trapped particles, and we might expect that, by adding more particles, some of the new ones will get trapped and some will move about the system due to the repulsion against the trapped ones, the result of which is a partial trapping state. What our results show, in contrast to this expectation, is that with the addition of more particles their mutual repulsion will render all of them untrapped; i.e., by adding more particles, the ones already trapped are replaced by the new ones, which, in turn, will be replaced by other particles, and so on; the result is a no trapping state. This is a consequence of our choosing such small traps; for large ones, increasing φ will cause particles outside the trap to aggregate, leaving the region close to it at a smaller density [21].

Hence, we can state that, for a given φ and V_0, we have no trapping state for high B (small well); partial, or no, trapping for intermediate B; and, finally, total trapping for low B (or strong well). Also, we see again that high noise particles are more susceptible to being trapped with soft boundaries.

Let us return to the $D_r = 10^{-5}$ case. The MSD curves for this case follow trends similar to those seen for the other noise values. But we should be careful to interpret the data for the FTP and to correlate it to the corresponding MSD curves in this case: for instance, for $\varphi = 0.1$, we have normal diffusion for all B, but an FTP that is close to 1, indicating a complete trapping state. The issue here is that, given their

very low noise, they take very long times, longer than our simulation time, to change their motion direction appreciably; hence, when falling in a strong well, they take long times to reach the "escape routes"; they stick, as it were, to the maximum restoring force boundary. Nevertheless, they move in such boundaries, albeit very little [compare the magnitudes of the MSD curves of Fig. 1(a) for $B \leqslant 0.7$ to those for $B > 0.7$]. In Fig. 3(b), we have the average density field for $\varphi = 0.1$, $B = 0.4$, and $D_r = 10^{-5}$; the rings that form around the well centers are the consequence of the effect just described. Again, such rings were observed in Refs. [21,22], and their local structure is a triangular lattice. Here, given the size of the traps, we should not expect to see such symmetric arrangements, for they require a large number of trapped particles to occur.

B. Sorting in binary mixtures of distinct noise values

We have considered the diffusion and trapping phenomenon of active particles with a single noise. By following along the lines of Ref. [14], we study how we can separate a mixture of active particles with two distinct noise values. We consider the same model, but now the N particle system is a 50 : 50 mixture of particles with noise values D_{r1} and $D_{r2} > D_{r1}$. Since we have already characterized the relation between the diffusion regime and the trapped state, we concentrate here only on the FTP as the indicator of separation.

In Ref. [14], the authors showed that the efficiency of the sorting is enhanced by the disparity between the noise values of the particles in the mixture: the larger the latter, the better the former. Our simulations, on the other hand, show a more complicated scenario for sorting particles based on noise differences with soft traps; although there is a tendency for a better sorting based on this difference, the whole phenomenon depends, additionally, on the well size, B, and the overall density, φ. We show, in Fig. 6, the results for the FTP of two mixtures as a function of B for all φ, that illustrate the phenomenon. For the first mixture, we consider $D_{r1} = 10^{-5}$ and $D_{r2} = 10$; for the second, we choose $D_{r1} = 10^{-2}$ and $D_{r2} = 1.0$.

In order to have a good sorting, the FTP for one type should be considerably larger than the other. From Fig. 6, we see that this is achieved only in the following cases: for the first mixture at $\varphi = 0.2$, $B = 0.5$, and $\varphi = 0.3$, $B \leqslant 0.2$; for the second mixture, this feature is seen for $\varphi = 0.1$, $B = 0.1$ and 0.6, $\varphi = 0.2$, and $B = 0.3$ and 0.2. It is worth noticing that the results for $B \leqslant 0.4$ may be influenced by the deformity of the well, as pointed out earlier. Hence, we concentrate on the other cases, namely, $D_{r1} = 10^{-5}$, $D_{r2} = 10$, $\varphi = 0.2$, and $B = 0.5$; and $D_{r1} = 10^{-2}$, $D_{r2} = 1.0$, $\varphi = 0.1$, and $B = 0.6$.

Why does this scenario occur? Our results for a single noise system indicate that interactions between particles are crucial for them to overcome the maximum restoring force (see the dependence of the FTP on φ, Fig. 4) and escape the traps; also, similarly to what was reported in Refs. [21–23], particles are trapped at distinct radii (forming shells) related to the well minimum, and these radii grow for lower noise particles. In a mixture, if both types are trapped, they will be at distinct radii around the minima. Therefore, if these shells are far enough so that interactions between the particles of distinct

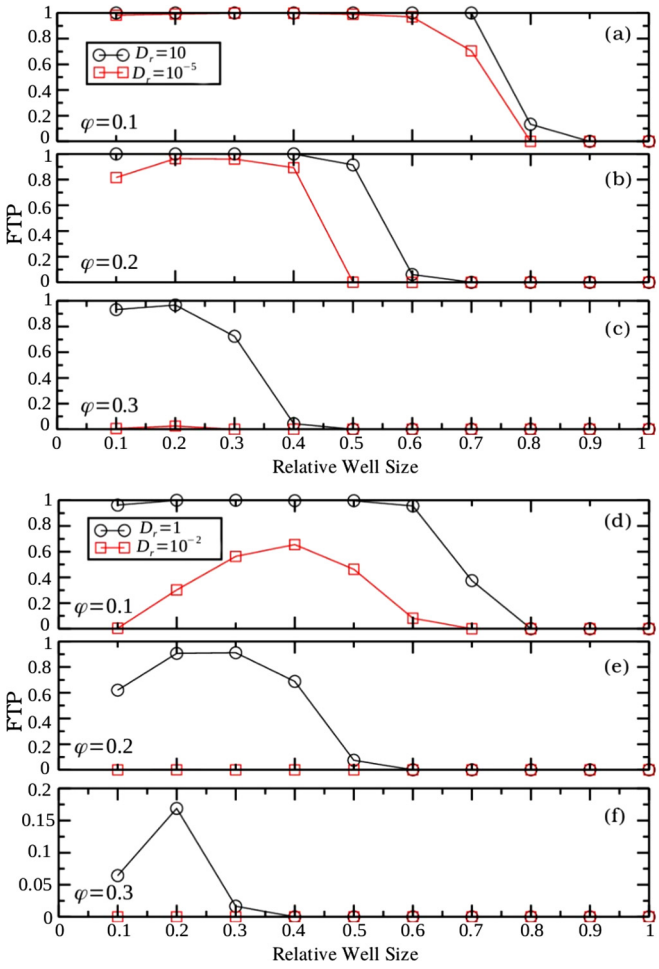

FIG. 6. The FTP for (a, d) $\varphi = 0.1$, (b, e) $\varphi = 0.2$, and (c, f) $\varphi = 0.3$. (a–c) $D_{r1} = 10^{-5}$ and $D_{r2} = 10$. (d–f) $D_{r1} = 10^{-2}$ and $D_{r2} = 1$.

noises are weak, they will behave as two isolated systems, with the trapping scenario given by our previous analyses. This is what occurs for the first mixture in the cases at $\varphi = 0.1$ and $B \leqslant 0.6$; in fact, larger noise particles in a mixture tend to be more trapped, i.e., to have a higher FTP as compared to the single noise value result, because they occupy shells closer to the minima, and, in order to escape a trap, would have to overcome not only the potential barrier but also the outer layer of lower noise particles in the same mixture. By this same reasoning, lower noise particles more easily escape the traps. For both mixtures, at all φ and $B \geqslant 0.8$, the FTP vanishes because the wells are too small to trap any particle (which also occurs for the single noise value system, see Fig. 4). For all other cases, we have either a poor or a good sorting.

This picture is corroborated by the data on the mean trapping radius $\langle r_{\text{trap}} \rangle$, shown in Fig. 7 as a function of time for all φ and $B = 0.5$, for the first mixture, and $B = 0.6$ for the second mixture. This quantity, the mean trapping radius, indicates the average distance the particles are from the nearest well minimum; its value is roughly the radius of the shell, while its variance is a rough measure of the width of the shell. Let us begin with the data for the first mixture, Fig. 7(a). For $\varphi = 0.1$ and 0.2, we see that the differences between the radii are 0.70 and 0.53, respectively; in both cases, there is the possibility of interactions, since these values

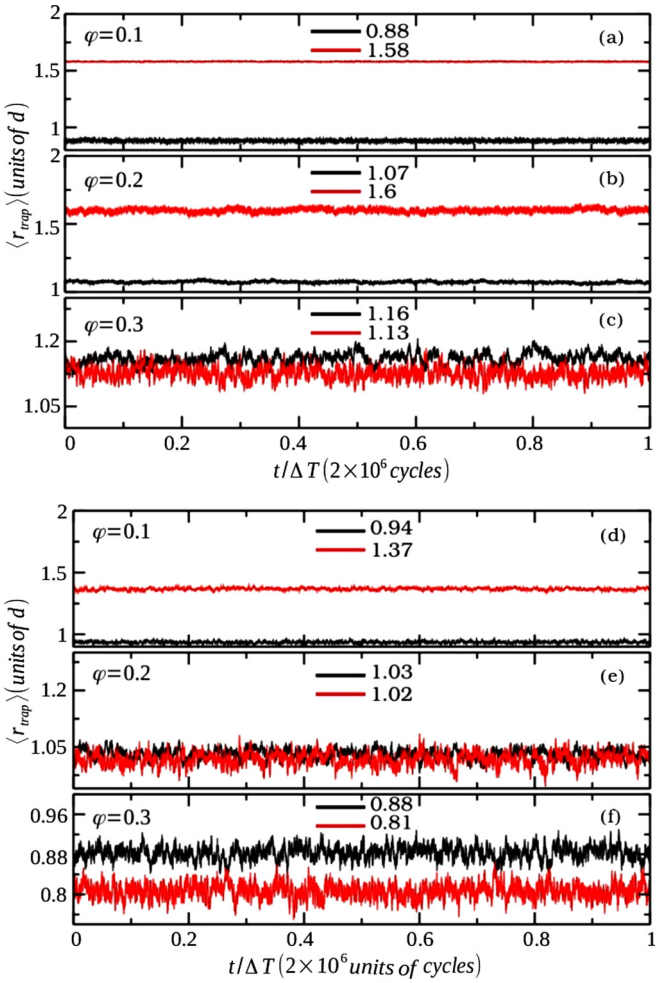

FIG. 7. Time-averaged radius trap over the whole simulation time for (a, d) $\varphi = 0.1$, (b, e) $\varphi = 0.2$, and (c, f) $\varphi = 0.3$. Upper panel: Mixture composed by particles with $D_r = 10$ (black) and 10^{-5} (red) in a well for $B = 0.5$. Bottom panel: Mixture composed by particles with $D_r = 1$ (black) and $D_r = 10^{-2}$ (red) in a well for $B = 0.6$. The horizontal axis is normalized by the simulation time in each case.

are less than one diameter, but only for $\varphi = 0.2$ we see a good sorting. We explain this feature by the smaller difference between the radii, which allow more frequent and intense particle interactions (they may overlap more strongly), and the fact that the low noise ones are very close to the maximum restoring force level, and any push from within the well may render them free. For $\varphi = 0.1$, given that we have fewer particles, they do not interact with the intensity needed for some to escape, hence we have a complete trapping state. For $\varphi = 0.3$, we have no trapping, and, given that we have more particles, they occupy roughly the same levels around the minima with strong fluctuations around the mean; hence, no particle stays for long within a single well.

In the second mixture, Fig. 7(b), the picture is similar: for $\varphi = 0.1$, particles have clearly distinct trapping radii, with a difference of 0.43, which allows for sorting for this mixture; in the other two densities, we have no trapping, with both having nearly equal trapping radii with strong fluctuations. In view of the previous results, we speculate that for a lower density the trapping radii difference would be larger, and we would have a complete trapping state.

We may summarize our observations as that in order to have sorting we need an appropriate density value for each mixture, so that interactions between species may be just enough to push the lower noise particles off the traps; if this parameter is lower or larger, we will have a complete trapping (insufficient interactions) or no trapping (too many interactions). This appropriate density value depends on the strength of the potential, the intensity of the repulsion between the particles, and the difference between their rotational noise values.

IV. CONCLUSIONS AND OUTLOOKS

We studied the diffusion and trapping of either a system of active particles with a single noise value or mixtures with equal proportions of active particles with two distinct noise values under the influence of an attractive periodic background. We called such attractive traps soft traps, in opposition to the previous study of this phenomenon in a V-shaped, rigid trap. In the single noise value cases, we showed that the diffusion regime is closely correlated to the trapping state: complete trapping corresponds to no diffusion or subdiffusion; partial or no trapping corresponds to normal diffusion. We observed that particles with lower noise values have more difficulty to escape from a trap, which is consistent with previous studies of active particles under the influence of soft traps [23,24]. We also studied how the diffusion and trapping regimes change with increasing density and observed that the relevant effect of increasing this quantity is to render all particles, except those of very high noise values, free; i.e., starting from some trapped state, the system will always reach a no-trapping regime.

For mixtures of particles with distinct noises, we studied the possibility to sort particles based on this difference. In contrast to a similar study in a hard V-shaped trap [14] we found that the noise difference alone is not enough to determine the sorting efficiency. Additionally, given the soft boundary, an appropriate density (not too small or too large) is needed to achieve an efficient separation, i.e., to trap only one type of particles. The separation of particles occurs because, for given background strength, noise difference, and density, the particles become trapped in a well at specific radii [23], the trapping radii, which decrease for higher noise. Therefore, the difference between the trapping radii should allow interactions between particles so that those on the larger radius (typically, particles with lower noise values) may escape the trap. Despite the more complex scenario for particle sorting in soft traps, when compared to hard traps, it is still possible to draw efficient sorting strategies.

ACKNOWLEDGMENTS

This study was financed in part by the Coordenação de Aperfeiçoamento de Pessoal de Nível Superior - Brasil (CAPES) - Finance Code 001, Fundação Cearense de Apoio ao Desenvolvimento Científico e Tecnológico - Brasil (FUNCAP) - Grant No. 0447/2018 and Conselho Nacional de Desenvolvimento Científico e Tecnológico - Brasil (CNPq) - Grant No. 434910/2018-0.

[1] T. Vicsek, A. Czirók, E. Ben-Jacob, I. Cohen, and O. Shochet, Novel Type of Phase Transition in a System of Self-Propelled Particles, Phys. Rev. Lett. **75**, 1226 (1995).

[2] C. W. Reynolds, Flocks, herds, and schools: A distributed behavioral model, ACM Siggraph Computer Graphics **21**, 25 (1987).

[3] Y. Fily and M. C. Marchetti, Athermal Phase Separation of Self-Propelled Particles with no Alignment, Phys. Rev. Lett. **108**, 235702 (2012).

[4] E. Mani and H. Löwen, Effect of self-propulsion on equilibrium clustering, Phys. Rev. E. **92**, 032301 (2015).

[5] C. Kreuter, U. Siems, P. Nielaba, P. Leiderer, and A. Erbe, Transport phenomena and dynamics of externally and self-propelled colloids in confined geometry, Eur. Phys. J. Special Topics **222**, 2923 (2013).

[6] S. E. Spagnolie, G. R. Moreno-Flores, D. Bartolo, and E. Lauga, Geometric capture and escape of a microswimmer colliding with an obstacle, Soft Matter **11**, 3396 (2015).

[7] M. B. Wan, C. J. Olson Reichhardt, Z. Nussinov, and C. Reichhardt, Rectification of Swimming Bacteria and Self-Driven Particle Systems by Arrays of Asymmetric Barriers, Phys. Rev. Lett. **101**, 018102 (2008).

[8] P. Galajda, J. Keymer, P. Chaikin, and R. Austin, A wall of funnels concentrates swimming bacteria, J. Bacteriol. **189**, 8704 (2007).

[9] U. Choudhury, A. V. Straube, P. Fischer, J. G. Gibbs, and F. Höfling, Active colloidal propulsion over a crystalline surface, New J. Phys. **19**, 125010 (2017).

[10] M. Balvin, E. Sohn, T. Iracki, G. Drazer, and J. Frechette, Directional Locking and the Role of Irreversible Interactions in Deterministic Hydrodynamics Separations in Microfluidics Devices, Phys. Rev. Lett. **103**, 078301 (2009).

[11] H. E. Ribeiro and F. Q. Potiguar, Active matter in lateral parabolic confinement: From subdiffusion to superdiffusion, Physica A **462**, 1294 (2016).

[12] X. Shen, Marcos, and H. C. Fu, Traction reveals mechanisms of wall effects for microswimmers near boundaries, Phys. Rev. E. **95**, 033105 (2017).

[13] A. Kaiser, H. H. Wensink, and H. Löwen, How to Capture Active Particles, Phys. Rev. Lett. **108**, 268307 (2012).

[14] N. Kumar, R. K. Gupta, H. Soni, S. Ramaswamy, and A. K. Sood, Trapping and sorting active particles: Motility induced separation and smectic defects, Phys. Rev. E **99**, 032605 (2019).

[15] A. Ashkin, J. M. Dziedzic, J. E. Bjorkholm, and S. Chu, Observation of a single-beam gradient force optical trap for dielectric particles, Opt. Lett. **11**, 288 (1986).

[16] F. Q. Potiguar and R. Dickman, Colloids in a periodic potential: Driven lattice gas in continuous space, Phys. Rev. E **76**, 031103 (2007)

[17] A. M. Lacasta, J. M. Sancho, A. H. Romero, and K. Lindenberg, Sorting on Periodic Surfaces, Phys. Rev. Lett. **94**, 160601 (2005).

[18] K. Ladavac, K. Kasza, and D. G. Grier, Sorting mesoscopic objects with periodic potential landscapes: Optical fractionation, Phys. Rev. E. **70**, 010901(R) (2004).

[19] A. van der Horst, P. D. J. van Oostrum, A. Moroz, A. van Blaaderen, and M. Dogterom, High trapping forces for high-refractive index particles trapped in dynamic arrays of counter-propagating optical tweezers, Appl. Opt. **47**, 3196 (2008).

[20] P. T. Korda, M. B. Taylor, and D. G. Grier, Kinetically Locked-In Colloidal Transport in an Array of Optical Tweezers, Phys. Rev. Lett. **89**, 128301 (2002).

[21] W. Yang, V. R. Misko, J. Tempere, M. Kong, and F. M. Peeters, Artificial living crystals in confined environment, Phys. Rev. E **95**, 062602 (2017).

[22] W. Yang, V. R. Misko, F. Marchesoni, and F. Nori, Colloidal transport through trap arrays controlled by active microswimmers, J. Phys.: Condens. Matter **30**, 264004 (2018).

[23] A. Potosky and H. Stark, Active Brownian particles in two-dimensional traps, Europhys. Lett. **98**, 50004 (2012).

[24] L. Caprini, U. M. E. Marconi, A. Puglisi, and A. Vulpiani, Active espace dynamics: The effect of persistence on barrier crossing, J. Chem. Phys. **150**, 024902 (2019).

[25] A. Geiseler, P. Haenggi, and G. Schmid, Kramers escape of a self-propelled particle, Eur. Phys. J. B **89**, 175 (2016).

[26] E. Woillez, Y. Zhao, Y. Kafri, V. Lecomte, and J. Tailleur, Activated Escape of a Self-Propelled Particle from a Metastable State, Phys. Rev. Lett. **122**, 258001 (2019).

[27] K. Malakar, A. Das, A. Kundu, K. V. Kumar, and A. Dhar, Steady state of an active Brownian particle in two-dimensional harmonic trap, Phys. Rev. E **101**, 022610 (2020).

[28] C. Reichhardt and C. J. Olson, Novel Colloidal Crystalline States on Two-Dimensional Periodic Substrates, Phys. Rev. Lett. **88**, 248301 (2002).

[29] M. Brunner and C. Bechinger, Phase Behavior of Colloidal Molecular Crystals on Triangular Light Lattices, Phys. Rev. Lett. **88**, 248302 (2002).